COMPUTER MODELING OF RADIATION EFFECTS

N. B. Ouchi

Radiation Effect Analysis Group, Division of Environment and Radiation Sciences, Nuclear Science and Engineering Directorate, Japan Atomic Energy Agency, Tokai, Ibaraki 319-1195, Japan
Email: ouchi.noriyuki@jaea.go.jp

ABSTRACT

Biological effects of low-dose radiation are studied by computational methods. Assessing the risks of low-dose radiation, i.e. radiation-induced cancer, is becoming important in the study of public health because of the many different types of exposures, medical exposures, and from radiation protection viewpoints. In general, radiation effects arise from damage done to DNA by ionizing radiation. Therefore, examining effects from the initial DNA damage to the risk assessment is a problem with a very wide spatiotemporal scale. We are studying this problem by dividing it into three parts: 1) the DNA strand is broken by ionizing radiation, 2) DNA lesion repair, and 3) the process of cell carcinogenesis and tumorigenesis. In this paper, we mainly focus on the third part, the study of modeling and simulation of cell carcinogenesis.

Keywords: Computer simulation, Model, Carcinogenesis, Tumorigenesis, Multi-stage model

1 INTRODUCTION

In recent years, the importance of risk assessment of radiation exposure, especially at low doses, is becoming more important from many view points, i.e. medical exposure, radiation protection, cancer risk for astronauts, airline navigators, and workers in the nuclear industry. We see that one of the major difficulties of the problem is its large spatio-temporal scales, as shown in Figure 1. Radiation effects on humans take place initially in a very small region (~10^{-9}m) at a very short time (~10^{-9}s) interval. Following that, these small "effects" produce gene-mutations, and the accumulation of gene-mutations transforms normal cells into cancer cells (UNSCEAR, 2000). However, the risk estimation of the radiation is based mainly on a so-called dose-response curve from epidemiological studies. An epidemiological study needs a large number of samples to get statistically significant data although in practice it is difficult to obtain such a large number of samples in the area of low dose radiation risks. It is also well known that the epidemiological data are strongly dependent on life styles and generations and life times of the considered populations; therefore the validity of their application to other ages and life times is still unclear. On the other hand, new biological findings have substantially increased our understanding of the mechanisms of low dose radiation effects. In recent years, the necessity for a new risk assessment based on biological mechanisms has widely evolved. Computer modeling and simulation are quite effective in clarifying the mechanism of radiation effects because a phenomenon taking place in a small region

in a very short time can be observed, which is difficult to examine by experimental approaches. As explained above, the size of the problem is very large, and thus we classified it into three different sized problems, from phenomenological view points: 1) DNA strand breakage by ionizing radiation (Watanabe & Saito, 2002), 2) DNA lesion repair (Bunta, Laaksonen, Pinak, & Nemoto, 2006), and 3) the process of cell carcinogenesis and tumorigenesis. Hereafter, we mainly focus on the third problem, the modeling and simulation of cell carcinogenesis and tumorigenesis.

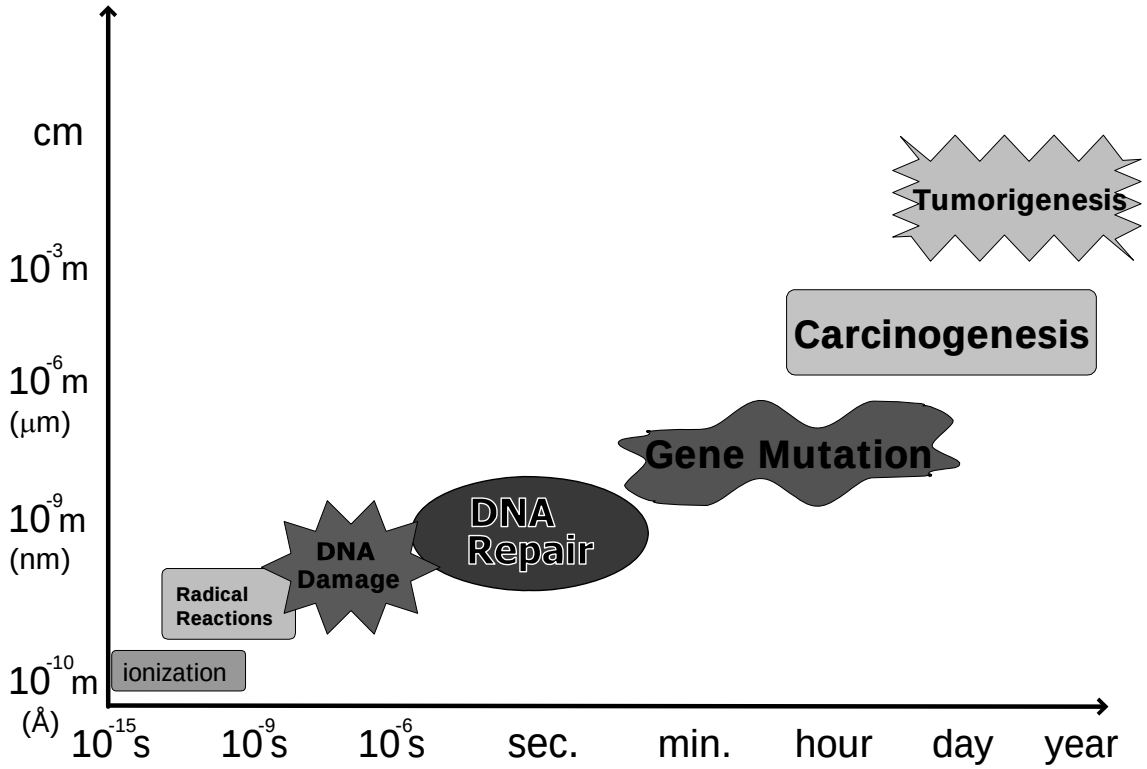

Figure 1. Schematic explanation of the spatiotemporal relationship of the problem. We see a very small initial event becoming sequentially a large-scale phenomenon. Scales depicted in the axis are approximate.

2 MODEL

Our model for cell carcinogenesis and tumorigenesis is composed of many cells, which have flexible free surfaces and internal biological mutation processes. Cells are classified into four types (normal, initiated, promoted, and cancer) by their stage of carcinogenesis. The process of carcinogenesis is described by intracellular biological (mutation) dynamics and extra cellular physical dynamics (cell movement), and therefore we modeled it by a combination of both. For the physical dynamics part of the model, we use the cellular large-*Q* Potts model (CPM), which is based on a biological hypothesis by Steinberg (1970). The CPM assigns a spin σ_{ij} to each lattice site (i, j), and packed sites that have the same spin number define a cell. Each cell has an associated cell type, τ. Figure 2 shows the schematic explanation of the formation rule of a cell of our model (Ouchi, Glazier, Rieu, Upadhyaya, & Sawada, 2003).

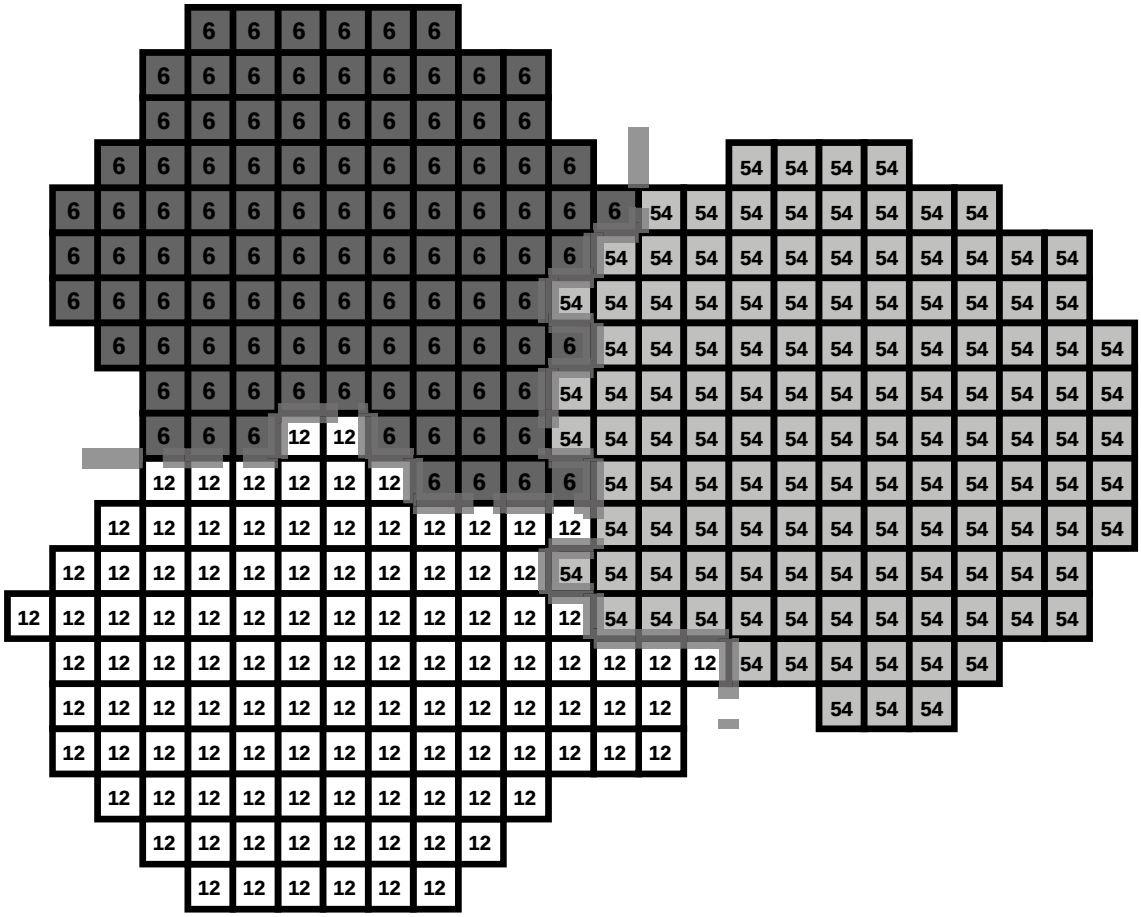

Figure 2. Schematic explanation of the cell configuration of the simulation. The numbers in the lattice show $\sigma_{ij,}$ and each group of σ_{ij} defines a cell. The colors of each cell define the cell type, in this case, the stage of the cellτ. A fat line in the figure shows the bonding side of the cell.

As a stage of carcinogenesis, we introduce four cell types: τ_i, where τ_1 denotes a normal cell, τ_2 an initiated cell, τ_3 a promoted cell, and τ_4 a cancer cell. In the simulation, we calculate the total energy of the system, H, from:

$$H = \sum_{(i,j)} J_{\tau\tau'}(1-\delta_{\sigma,\sigma'}) + \left\{ \lambda_1 \sum_{\sigma} (a(\sigma) - A_\tau)^2 + \lambda_2 \sum_{\sigma} (l(\sigma) - l_\tau)^2 \right\} (1-\delta_{\tau,m}),$$

where $a(\sigma)$ and $l(\sigma)$ are respectively the area and perimeter of the cell σ, $\lambda_1$and λ_2 are the elasticity parameters, A_τ the target cell area, and l_τ the target perimeter. $J_{\tau\tau'}$ is the adhesive energy between cell τ and cell τ'. We also denote medium as a cell type $\tau=m$. At each step, we use the Monte Carlo method to simulate cell group movement. Using this CPM formalism, we can simulate many of the cell group dynamics, e.g., the cell sorting process (Grazier & Graner, 1993).

For the intracellular dynamics, we adopt a simple multi-stage stochastic state transition equation based on the molecular biological finding of Fearon and Vogelstein (1999), which also includes the probability of cell death and cell division (Fig. 3). Thus the parameters of the intracellular dynamics can be classified into three categories: cell transition, cell death, and cell proliferation. In our model, complicated mass effects of the cell group are handled by the extracellular dynamics, and therefore included intracellular dynamics are very simple.

In the next section, we give some simulation results.

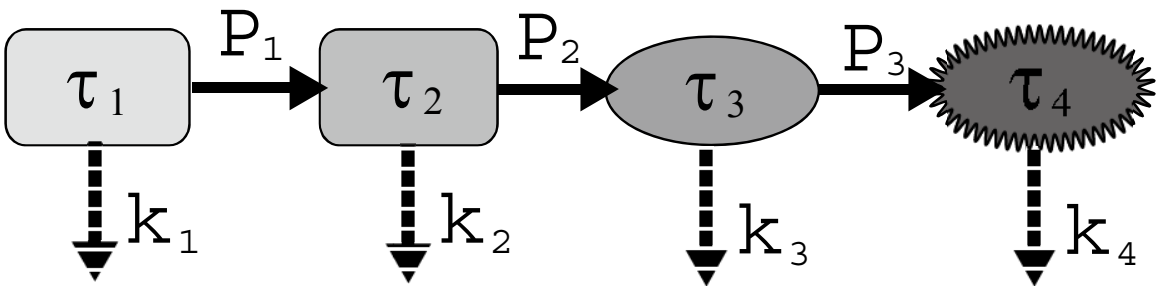

Figure 3. Schematic explanation of the intracellular dynamics of our model. In this figure, τ_1, τ_2, τ_3, τ_4 show the normal, initiated, promoted, and cancer cell stages respectively, P_1, P_2, P_3 are the mutation rates, in a broad sense, of each stage, and k_1, k_2, k_3, k_4 are the cell death rates for each stage. If the cell area exceeds some threshold value, $a(\sigma) > a_c$, then cell division occurs.

3 SIMULATION RESULTS

For the initial state of the simulation, we choose normal cells with 0.2% initiated cells. The total number of cells is about 260. We have numerically studied our model by changing the state transition and cell death parameters, P_i and k_i. Figures 4(A) – 4(C) show typical cell population dynamics of the model. We obtained 3 distinguishable state change dynamics, called type A, type B, and type C. As shown in Figure 4(A), the population of the normal cells N_1 remains relatively steady with time, $dN_1/dt = 0$, and the population of the cancer cells N_4 is nearly zero, $N_4 \approx 0$. Thus the state can be thought to be in equilibrium, and we get no tumor at this state. On the contrary, the formation of a tumor is seen in type B and type C states. The primary difference between type B and type C states is the tumor growth rate and decrease of normal cells. In the type B state, we see exponential growth of the tumor and exponential decrease of the normal cells. In the type C state, the growth rate of the tumor appears to be linear, and moreover the population of the normal cells is linearly decreasing, $dN_4/dt=\kappa_4$, $dN_1/dt=-\kappa_1$, where κ_1 is the decrement coefficient and κ_4 the growth rate coefficient. Temporal snapshots of the simulation are shown in Figure 5. Starting from the same initial condition, we have obtained these 3 distinguishable states, explained above. We can see the clear difference between type B and type C states in the middle snapshots, and the population of the cells with promoted stage in the type B state is larger than that in type C. Further research which increases the variety of parameter sets and analysis of the parameter dependency is now in progress.

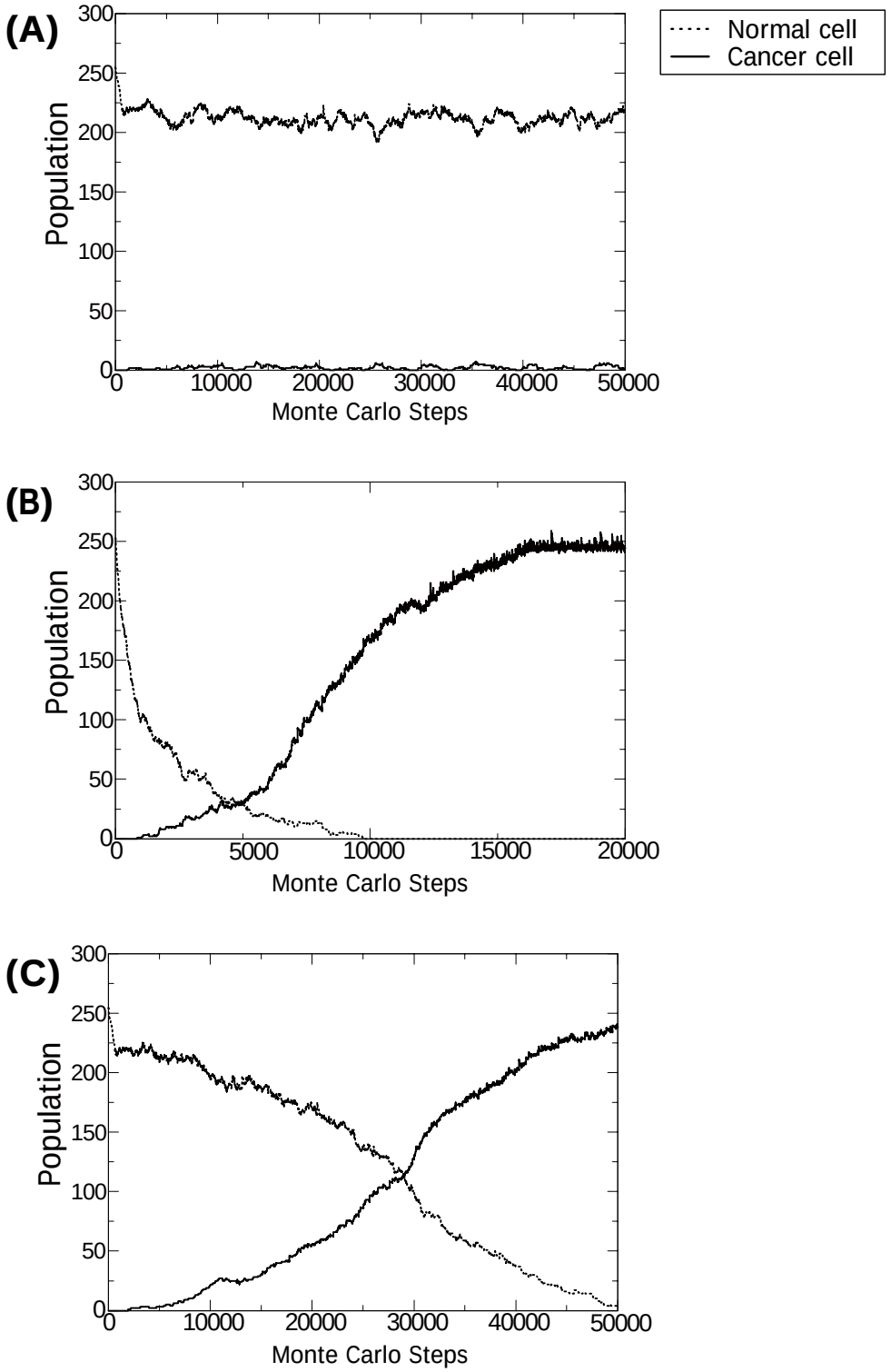

Figure 4. Collection of time series plots of the population for normal cells (dotted line) and cancer cells (solid line). Figures (A), (B), and (C) are the plots of type A, type B, and type C respectively. The saturation of the cancer cell growth rate in figure (B) comes from the limitation of the system size.

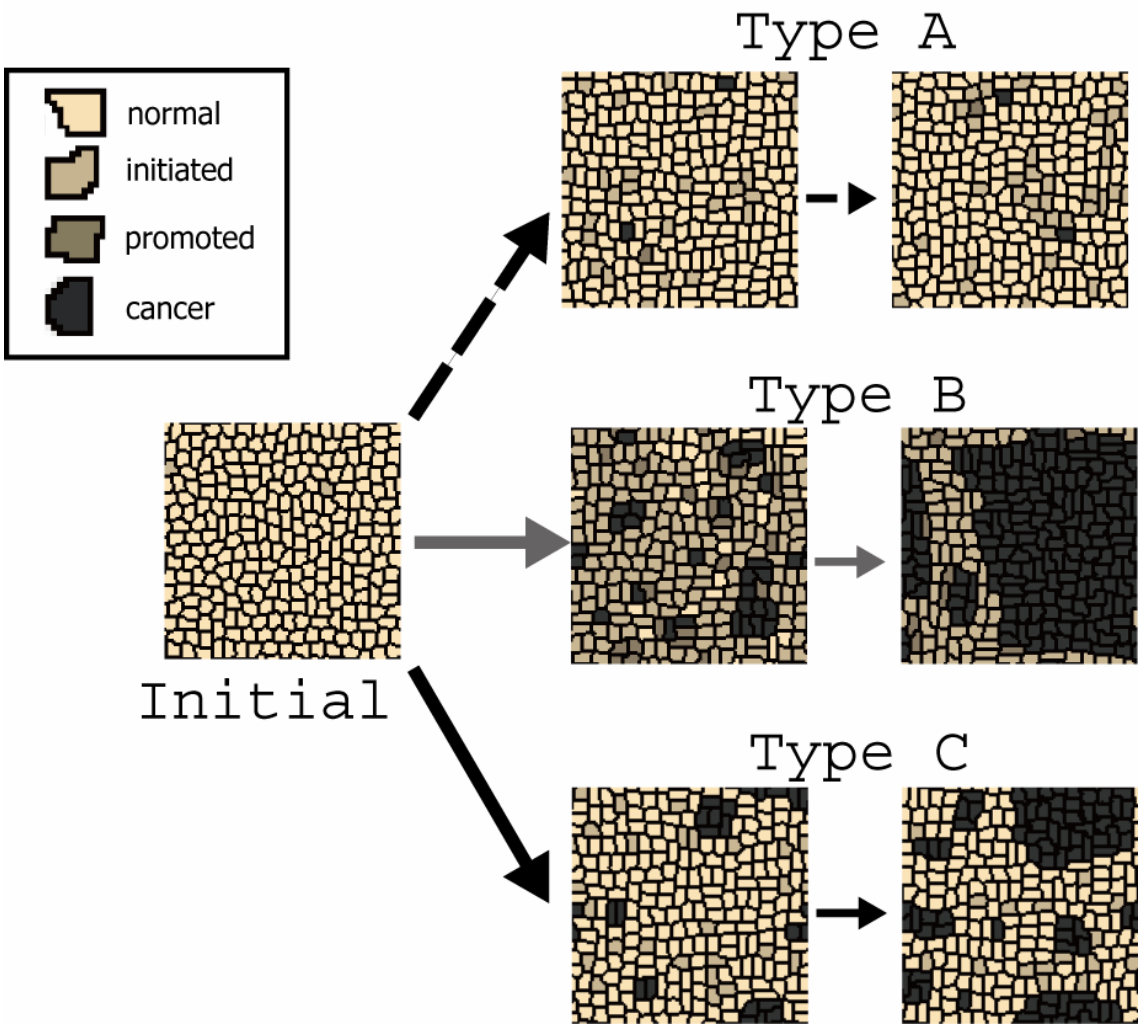

Figure 5. Snapshots of the simulation for each state. Arrows in the figure show directions of the simulation time. We have simulated these states using the same initial conditions.

4 CONCLUSION

We have modeled a process of tumorigenesis using CPM with simple intracellular dynamics. The dynamical states are classified into three by the population dynamics of the normal cells and cancer cells: steady equilibrium (type A), exponential (type B), or linear (type C); however we need to study further the statistical analysis of the coefficients κ_4, κ_1 and the functional structure of exponential dynamics. Moreover, the relation between these dynamics and the parameters needs more investigation. From the simulation results of this model, a parameter region where tumors did not grow is suggested. Within this model, we can investigate morphological aspects of the tumor growth process, one of the important features of this model. In the present paper, we focused mainly on the result of the three obtained states and their condition, while more extensive parameter space search and statistical analysis need further investigation.

5 ACKNOWLEDGEMENTS

I would like to thank Group Leader Dr. K. Saito for stimulating discussions and encouragement and also thank all the other group members for many useful discussions. This work is partially supported by KAKENHI (18700294) and the Budget for Nuclear Research of the Ministry of Education, Culture, Sports, Science, and Technology based on screening and counseling by the Atomic Energy Commission.

6 REFERENCES

Bunta, J. K., Laaksonen, A., Pinak, M., & Nemoto, T. (2006) DNA strand break: Structural and electrostatic properties studied by molecular dynamics simulation. *Comp. Biol. And Chem. 30*, 112-119

Fearon, E. R. & Vogelstein, B. (1999) A Genetic Model for Colorectal Tumorigenesis. *Cell 61*, 759-767

Grazier, J.A. & Graner, F. (1993) Simulation of the differential adhesion driven rearrangement of biological cells. *Phys. Rev. E 47*, 2128-2154

Ouchi, N. B., Glazier, J. A., Rieu, J. P., Upadhyaya, A., & Sawada, Y. (2003) Improving the realism of Potts model in simulations of biological cells. *Physica A 329*, 451

Steinberg, M.S. (1970) Does differential adhesion govern self-assembly process in histogenesis? Equilibrium configurations and the emergence of a hierarchy among populations of embryonic cells. *J. Exp. Zool. 173*, 395-434

UNSCEAR (Eds.) (2000) *Biological Effects at Low Radiation Doses – Models, Mechanisms and Uncertainties, Annex 1*, United Nations

Watanabe, R. & Saito, K. (2002) Monte Carlo simulation of strand-break induction on plasmid DNA in aqueous solution by monoenergetic electrons. *Radiat. Environ. Biophys. 41*(3), 207-15.